TENSILE LOADS IN POROUS ROTATING ASTEROIDS WITH ARTIFICIAL CAVERNS. T. I. Maindl[1], C. M. Schäfer[2], B. Loibnegger[1] and R. Miksch[1], [1]Department of Astrophysics, University of Vienna, Austria, thomas.maindl@univie.ac.at, [2]Institut für Astronomie und Astrophysik, Universität Tübingen, Germany.

Introduction: In a previous study [1] we estimated the necessary spin rate of a mined asteroid hosting a cylindrical space station with artificial gravity and estimated its required material strength deploying two simplified analytical models. Applying these models to fictitious, yet realistic rocky near-Earth asteroids resulted in material strengths comparable to tensile and shear strengths of basalt [1]. Here we present results of a series of smooth particle hydrodynamics (SPH) simulations of a typical configuration with varying porosity of the parent body and compare the SPH results which are based on solid body continuum mechanics to the analytical model predictions.

Models and scenarios: We assume a cylindrical cavern of radius r_c and height h_c which is in its entirety inside a spheroidal parent body with semi-axes a and b, respectively (see Fig. 1). In order to achieve artificial gravity g_c on the lateral cylinder surface, the asteroid has to rotate at a rate $\omega = (g_c/r_c)^{1/2}$ about the y axis. Here, we will assume $g_c = 0.38\ g_{Earth} \approx 3.73$ m s^{-2} (see [1, 2]).

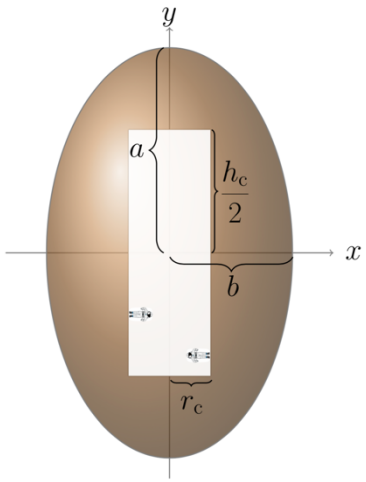

Figure 1. Geometry of the asteroid (cross section).

In an earlier study [1] we provided analytical estimates of the material loads based on two force models assuming a rigid and homogeneous rotating asteroid with a cylindrical cavern. While model 1 estimates the tensile stress acting on the symmetry (xy) plane, model 2 gives the tensile and shear stress working towards removing the "mantle" outside the space station due to the centrifugal force acting on material with $x^2 + z^2 \geq r_c^2$, and $|y| \leq \frac{1}{2}h_c$ (cf. Fig. 1). For the data given in Table 1 and basaltic rock of different porosity, the models predict material loads as given in Table 2. For competent rock, the loads are of basalt's tensile and shear strengths' order of magnitude (about 8–36 MPa, [3, 4]).

Table 1. Scenario parameters.

a [m]	b [m]	r_c [m]	h_c [m]	g_c [g_{Earth}]	ω [rad s^{-1}]	ω [rpm]
250	195	125	300	0.38	0.173	1.65

Here we present numerical simulations to test the analytical predictions and to constrain stability limits for mined asteroids with a substantial cavern. These simulations are based on the parameters given in Table 1 and assume a homogeneous parent body. We are interested in the load distribution inside the asteroidal body and use an adapted version of our CUDA-parallel 3D (SPH) hypervelocity impact code [5, 6] which implements elasto-plastic continuum mechanics, the p-α porosity model [7, 8], and a tensorial correction for first-order consistency [9]. The material model used for this study is based on the Tillotson equation of state with parameters for basaltic rock as given in [8] and porosities varying between 0% (solid) and 75%. Each scenario's resolution is about 500k SPH particles. The asteroid is set to rotation at the beginning of the simulation and is allowed to equilibrate during a 200s time interval resolved in output frames every 0.5s.

Table 2. Material load predictions from analytic models 1 and 2 (see [1]) and different porosity.

Matrix density ρ_m [kg m^{-3}]	*Porosity*	*Bulk density* ρ [kg m^{-3}]	*Model 1 load* σ_1 [MPa]	*Model 2 load* σ_2 [MPa]
2700	0%	2700	3.4	2.2
2700	20%	2160	2.8	1.8
2700	50%	1350	1.7	1.1
2700	75%	675	0.86	0.56

Results: As indicator for material load we deploy the von Mises stress $\sigma_e = (3J_2)^{1/2}$ with the second invariant of the deviatoric stress tensor J_2 which – expressed in terms of the regular stress tensor σ_{ij} – reads

$$J_2 = [\ (\sigma_{11}-\sigma_{22})^2 + (\sigma_{22}-\sigma_{33})^2 + (\sigma_{33}-\sigma_{11})^2] / 6 + \sigma_{12}^2 + \sigma_{23}^2 + \sigma_{31}^2. \quad (1)$$

After the SPH scenarios equilibrate they result in a stress pattern inside the rotating asteroid. Figure 2 shows snapshots of this σ_e stress pattern in the *xy* symmetry plane of the asteroid for the different material porosities. From a qualitative perspective, the patterns look similar, the biggest stresses occur at the corners of the cylinder and extend to the surface. Compared to the analytical model, the stress magnitude drops with increasing porosity in a more pronounced way (cf. the scale of the color bars) – while solid material results approximately resemble the figures in Table 2, porous material yields significantly lower σ_e values, deviations reaching one order of magnitude in the 75% porous case (cf. Table 2).

Conclusions: Our results show that both the analytical and numerical models predict the feasibility of using hollowed-out asteroids as parent bodies for potential space stations inside. Rotation rates providing sufficient artificial gravity result in material loads in the order of or less than the assumed material strength of rocky bodies.

While simple analytical models provide reasonable estimates for a limited number of cases thorough studies involving numerical simulations are necessary for obtaining accurate material loads determining the stability of the subject configurations. In the future we plan to deploy more accurate material models and to study realistic material and mass distributions in asteroids that may be candidates for mining and housing space stations in their interior.

Acknowledgements: TIM, BL, and RM received seed funding from the Dubai Future Foundation through Guaana.com open research platform. The authors acknowledge support by the High Performance and Cloud Computing Group at the Zentrum für Datenverarbeitung of the University of Tübingen, the state of Baden-Württemberg through bwHPC and the German Research Foundation (DFG) through grant no INST 37/935-1 FUGG and FWF Austrian Research Fund under project S11603-N16.

References: [1] Maindl T. I. et al. (2019) *FrASS,* subm. [2] Harris L. R. et al. (2014) *PLoS ONE, 9,* e106207. [3] Karaman K. et al. (2015) *J. Southern African Inst. of Mining and Metallurgy, 115,* 185–192. [4] Stowe R. L. (1969) *Army Eng. Waterways Exp. Station Vicksburg, Misc. paper,* C-69-1. [5] Maindl T. I. et al. (2013) *AN, 334,* 996–999. [6] Schäfer C. et al. (2016) *A&A, 590,* A19. [7] Jutzi M. et al. (2008) *Icarus, 198,* 242. [8] Haghighipour N. et al. (2018) *ApJ, 855,* 60. [9] Schäfer C. et al. (2007) *A&A, 470,* 733.

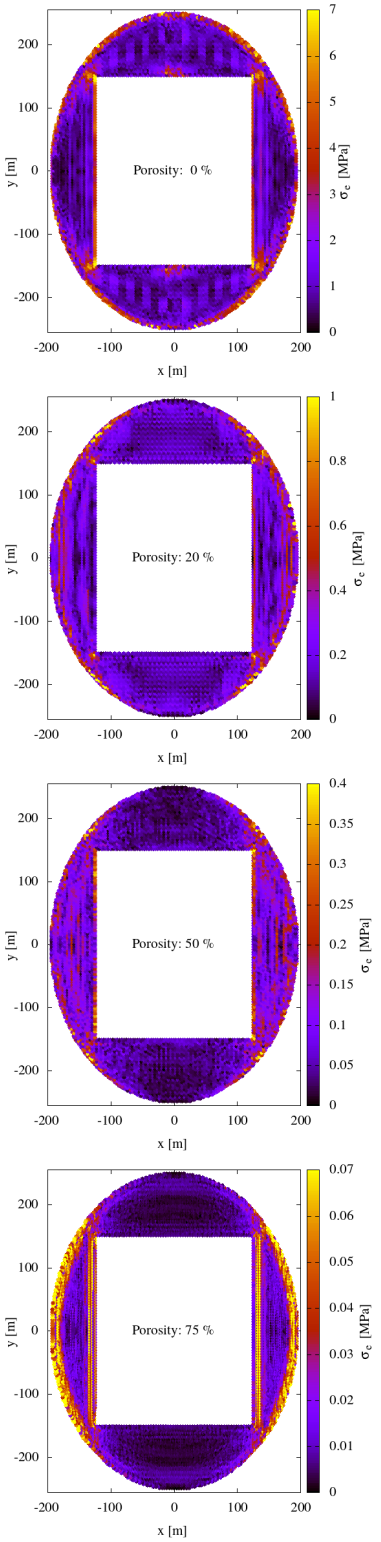

Figure 2. Color coded pattern of σ_e in the *xy* symmetry plane of the rotating asteroid. The assumed material porosity is indicated in the center.